

ORIGINAL ARTICLE

Stabilization of polystyrene thin films by introduction of a functional end group

Shinichiro Shimomura¹, Manabu Inutsuka¹, Koichiro Tajima², Masaaki Nabika², Satoru Moritomi², Hisao Matsuno¹ and Keiji Tanaka^{1,3}

The thin film stabilities of ω -*N*-(3-(dimethylamino)propyl)propylamide-terminated polystyrene (PS-N) and its blends with conventional polystyrene (PS-H) supported on silicon wafers with a native oxide layer were examined. Whereas a 20-nm-thick film of PS-H with a number-average molecular weight of ~ 50 k decomposed at 423 K, a comparable PS-N film and blended films containing a PS-N fraction of > 40 wt% were stable. Although the local conformation of chains at the substrate interface was not the same for PS with and without the functional end group, the glass transition temperature at the interface was identical for both PS-H and PS-N. The residual adsorbed layer on the substrate after washing the films with a good solvent was thicker for PS-N than for PS-H. This implies that end functionalization, rather than segmental dynamics, affects chain movement on a large scale.

Polymer Journal (2016) 48, 949–953; doi:10.1038/pj.2016.58; published online 8 June 2016

INTRODUCTION

Polymer composites containing inorganic nanofillers have been widely used in a variety of engineering fields.^{1–13} The performance and functionality of the composites are closely related to the quality of the interface between the polymer and the inorganic material. If the interaction between them is attractive, and the interface is well defined, then the fillers are dispersed homogeneously, and the reinforcement is effective.

We have previously studied the local conformation of a polystyrene (PS) film at the interface with an inorganic solid¹⁴ by sum-frequency generation (SFG) vibrational spectroscopy^{15–18} and noted that it is strongly dependent on the method of film preparation.¹⁴ It should be emphasized that the chain orientation at the interface was not well relaxed even at temperatures above the bulk glass transition temperature (T_g). This finding was in good accordance with the idea of an interfacial dead layer in terms of mobility^{19–21} as well as our parallel proposal that the T_g increases in close proximity to the substrate interface.^{22,23} These findings should prove important in the design of polymer composite interfaces.

To improve the interface affinity, reactive compounds such as silane coupling agents and ammonium salts have been used as surface treatments for silica fillers and clays, respectively.^{24–26} The introduction of functional groups onto polymer chains is also effective.^{27,28} However, at the present time it is unclear what effect such an interfacial modification has on the polymer structure and dynamics at the interface. This is perhaps one reason why perfect control of the interfacial interaction between the polymer and the inorganic material has not yet been achieved.

In this study, a thin film of terminally functionalized PS at an inorganic interface, where information concerning the interface is enhanced because of the large ratio of the interfacial area to the total volume,^{29–38} is characterized. This enables us to visualize polymer behavior at interfaces with inorganic solids and thus develop better strategies for the interfacial design of polymer composites.

EXPERIMENTAL PROCEDURE

Materials

Two types of PS, conventional and terminally functionalized, were used. The conventional PS (PS-H) was synthesized via anionic polymerization using secondary butyl (*sec*-Bu) lithium and methanol as the initiator and terminator, respectively. ω -*N*-(3-(dimethylamino)propyl)propylamide-terminated polystyrene (PS-N) was also synthesized anionically. Figure 1 shows the chemical structures of PS-H and PS-N. The number-average molecular weight (M_n) of PS-H was 56.5k, and the molecular weight distribution (M_w/M_n), where M_w is the weight-average molecular weight, was 1.07. The M_n and M_w/M_n of PS-N were 41k and 1.4, respectively. Deuterated PS-N (*d*-PS-N) with an M_n of 32k and an M_w/M_n of 1.6 was also synthesized (see Supplementary Figure S1a in the Supplementary Information), in which the functional end group of the polymer was not deuterated. The bulk T_g s of PS-H, PS-N and *d*-PS-N, determined by differential scanning calorimetry (Exstar6000 DSC6220, Hitachi High-Tech Science Corp., Tokyo, Japan), were 377, 376, and 376 K, respectively.

Characterization of thin films

Thin films of PS on clean silicon wafers with a native oxide layer were prepared by spin-coating from toluene solutions. The thickness of the PS films was 20 nm. The thermal stability, or dewetting behavior, of the thin PS films was examined by optical microscopy (VHX-700F, Keyence Co., Ltd, Osaka, Japan)

¹Department of Applied Chemistry, Kyushu University, Fukuoka, Japan; ²Sumitomo Chemical Co., Ltd, Chiba, Japan and ³International Institute for Carbon-Neutral Energy Research (WPI-I2CNER), Kyushu University, Fukuoka, Japan
Correspondence: Dr H Matsuno or Professor K Tanaka, Department of Applied Chemistry, Kyushu University, 744 Motooka, Nishi-ku, Fukuoka 819-0395, Japan.
E-mail: h-matsuno@cstf.kyushu-u.ac.jp or k-tanaka@cstf.kyushu-u.ac.jp

Received 13 January 2016; revised 4 April 2016; accepted 5 April 2016; published online 8 June 2016

at elevated temperatures.^{29–33} The local conformation of the PS at the interface was examined by SFG. For this measurement, two spin-coated films with a thickness of 400 nm on a half-cylinder quartz prism and a flat quartz substrate were attached in a face-to-face geometry under vacuum at 393 K for 24 h. Thus, the polymer films had only a quartz interface. Details on the SFG measurements have been described in a previous report.¹⁸ The T_g near the substrate interface was determined by space-resolved fluorescence lifetime measurements.^{22,23} Polymer films containing a fluorescent probe, 6-(*N*-(7-nitrobenz-2-oxa-1,3-diazol-4-yl)amino)hexanoic acid (NBD), were prepared on LiNbO₃ prisms on which a SiO_x layer had been deposited. The NBD in the films was excited by a picosecond laser pulse with a wavelength of 430 nm, and the consequent fluorescence was detected by a streakscope. When the incident angle of the pulse was larger than the critical angle, the excitation pulse was totally reflected at the interface between the PS and the substrate. Information about the region near the substrate interface was derived on the basis of this evanescent wave excitation. Reflectivity measurements using X-rays with a wavelength of 0.154 nm as a light source (Smartlab, Rigaku Co., Ltd, Tokyo, Japan) were applied to the PS-H and PS-N films on silicon wafers; these were annealed under vacuum at 393 K for 24 h and then rinsed three times in toluene for 10 min, so that the thickness of the adsorbed polymer layer on the substrate³⁹ could be evaluated. The data were analyzed using Parratt32 software based on Parratt's algorithm, a freeware program developed by C Braun and available from the Hahn-Meitner Institute (Berlin, Germany).

RESULTS AND DISCUSSION

Thin film stability

Figure 2 shows optical micrographs of (Figure 2a) PS-H, (Figure 2b–e) blends of PS-H and PS-N (80/20, 60/40, 40/60 and 20/80 w/w) and (Figure 2f) PS-N films after annealing at 423 K for 1 h. The thickness

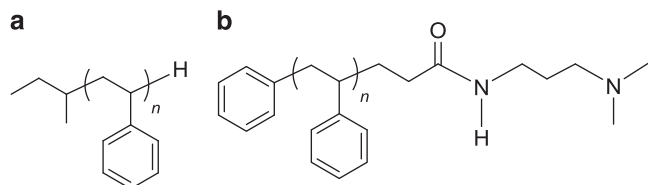


Figure 1 Chemical structures of (a) conventional polystyrene (PS-H) and (b) ω -*N*-(3-(dimethylamino)propyl)propylamide-terminated polystyrene (PS-N).

of all the films was set to be ~ 20 nm. The PS-H film decomposed upon annealing, as shown in panel (a). However, the PS-N film remained stable under these conditions, as shown in Figure 2f. Dewetting was not observed for the PS-N film, even at 473 K. If we postulate that the end group of the polymer chain was chemically bound to the substrate surface via hydrogen bonding between its amide/dimethyl amino groups and the silanol/siloxane groups on the surface of the Si wafer containing a native oxide layer, then the improved thermal stability for the thin PS-N film can be understood. In subsequent experiments, PS-N was blended with PS-H at various compositions to determine the extent to which chain end modification is effective in conferring stability to PS films. Whereas the PS-H film containing 20 wt% PS-N partially dewetted at 423 K (Figure 2b), the PS-H film containing more than 40 wt% PS-N remained intact (Figure 2c–e).

Interfacial chain conformation

SFG measurements were used to examine the aggregation state of the chains at the substrate interface. Figure 3 shows the spectra for the

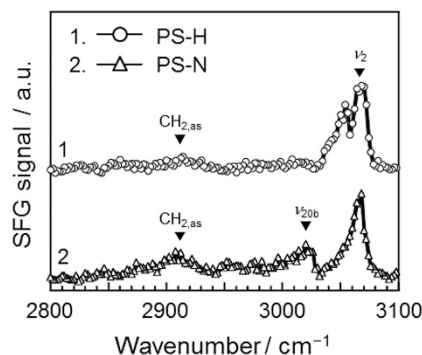


Figure 3 Sum-frequency generation (SFG) spectra for conventional polystyrene (PS-H) and ω -*N*-(3-(dimethylamino)propyl)propylamide-terminated polystyrene (PS-N) films at the quartz interface with the *ssp* polarization combination.

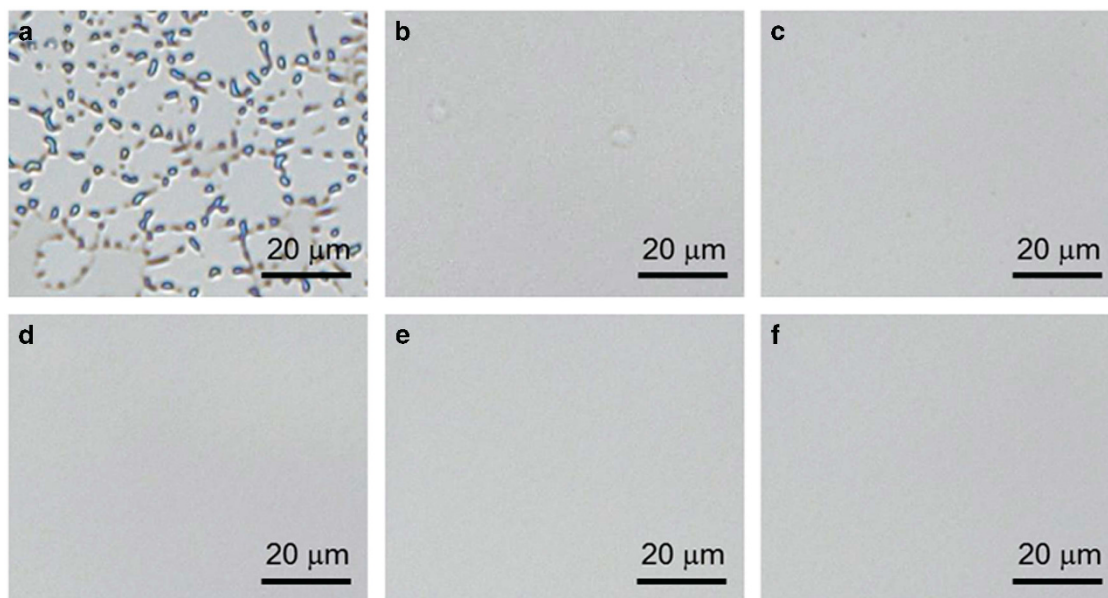


Figure 2 Optical micrographs of (a) conventional polystyrene (PS-H), (b) 80/20, (c) 60/40, (d) 40/60 and (e) 20/80 PS-H/PS-N blends and (f) ω -*N*-(3-(dimethylamino)propyl)propylamide-terminated polystyrene (PS-N) thin films annealed at 423 K for 1 h. All ratios are w/w.

PS-H and PS-N films supported on quartz with the *ssp* (SF output: *s*, visible input: *s*, and infrared input: *p*) polarization combination that provides information along the direction normal to the interface. In the case of PS-H, a weak peak was observed at $\sim 2910\text{ cm}^{-1}$. We had previously synthesized two different perdeuterated PSs (d_8 -PS) using either *sec*-butyl lithium or *n*-butyl lithium as initiators and methanol

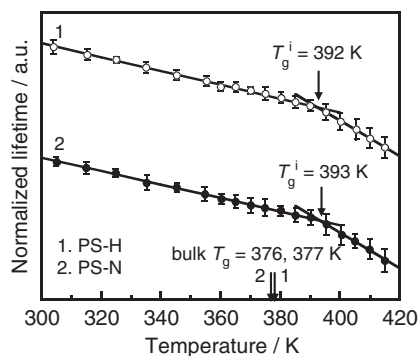


Figure 4 Temperature dependence of 6-*N*-(7-nitrobenz-2-oxa-1,3-diazol-4-yl)amino)hexanoic acid (NBD) lifetime at the substrate interface in conventional polystyrene (PS-H) and ω -*N*-(3-(dimethylamino)propyl)propylamide-terminated polystyrene (PS-N) films. Lifetime is normalized by the value obtained at room temperature.

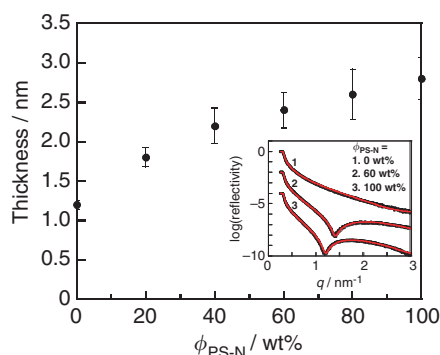


Figure 5 The ω -*N*-(3-(dimethylamino)propyl)propylamide-terminated polystyrene (PS-N) fraction ($\phi_{\text{PS-N}}$) dependence of thickness for the adsorbed layer on the substrate. Typical X-ray reflectivity (XR) curves for films with $\phi_{\text{PS-N}}$ of 0, 60 and 100 wt% are shown in the inset. Symbols and solid red lines in the inset denote experimental and calculated reflectivity, respectively.

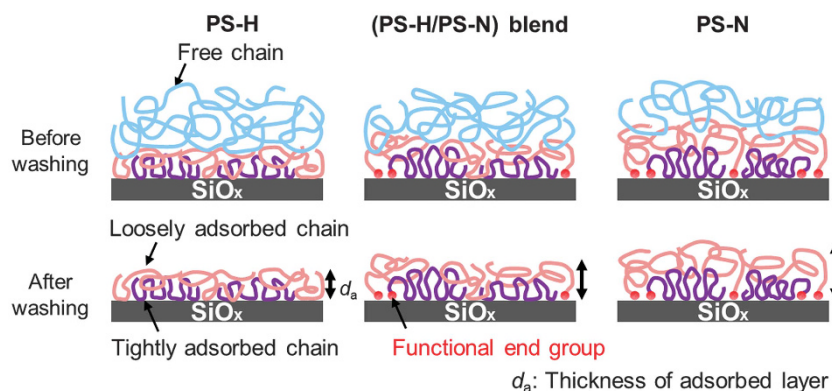


Figure 6 Schematic views of possible chain conformations in the interfacial region of thin films. Upper and lower rows show conformations before and after washing, respectively. PS-H, conventional polystyrene; PS-N, ω -*N*-(3-(dimethylamino)propyl)propylamide-terminated polystyrene.

as the terminator.^{18,40} By comparison with the SFG spectra for these d_8 -PSs, the peak at 2910 cm^{-1} was assigned as the antisymmetric C-H stretching vibration of the methylene groups ($\text{CH}_{2,\text{as}}$) in the initiator fragments. In the case of PS-N, a signal was also observed at 2910 cm^{-1} . Using *d*-PS-N for comparison, the peak was again assigned as $\text{CH}_{2,\text{as}}$, as shown in Supplementary Figure S1b. These findings clearly indicate that the functional end group of PS-N was aligned at the interface. Because the signal intensity of $\text{CH}_{2,\text{as}}$ was stronger for PS-N than for PS-H, it can be inferred that the population of end groups at the solid interface was higher for PS-N and/or that the extent of interfacial ordering of $\text{CH}_{2,\text{as}}$ was larger for PS-N.

An intense peak assignable to the ν_2 mode of the phenyl groups was observed at $\sim 3070\text{ cm}^{-1}$.^{41,42} The detection of SFG signals for the phenyl groups implies that the main chain was aligned along the in-plane direction because of the centrifugal force applied during the film preparation process.¹⁸ The introduction of the terminal group to PS altered the spectrum shape in the phenyl region from 3000 to 3100 cm^{-1} . The peak because of the ν_2 mode became sharper, and an additional peak appeared at 3020 cm^{-1} . These results indicate that the interfacial orientation of the phenyl rings of PS-N is different from that of PS-H. An increase in the amplitude ratio of ν_{20b} to ν_2 for PS-N implies that the phenyl rings are more tilted away from the normal direction.^{18,40,42,43} One possible explanation for this phenomenon is that greater distortion of the polymer chains during the spin-coating process occurs because the end groups are anchored to the substrate. Because the anchoring limits slippage of the chains on the substrate, the chains experience additional force.

Interfacial chain mobility

Based on the SFG study, there is little doubt that the functional terminal groups are bound to the substrate surface. The next question to address is whether the T_g at the substrate interface is elevated for PS-N. Figure 4 shows the temperature dependence of the fluorescence lifetime for the NBD dispersed in the PS-H and PS-N films. The analytical depth, calculated on the basis of the refractive index difference between PS and the substrate and using an incident angle θ of 74° for the excitation pulse, was 22.4 nm .²² Although this number was larger than the depth range in which the mobility gradient exists, the experimental result mostly reflects the chain mobility near the solid interface.²² This is because of the intensity of the electric field of the evanescent light exponentially decaying along the depth direction and thus being strongest at the outermost interface. In general, the lifetime decreased with increasing temperature because of the

manifestation of nonradiative pathways to the ground state. At temperatures above the T_g , segmental motion was released, and the slope of the temperature–lifetime curve changed because the dynamic environment surrounding the NBD changed at this temperature.²² This indicated that the T_g value at the interface could be determined from the inflection point of the temperature–lifetime curve. The interfacial T_g (T_g^i) for PS-N was 393 K, noticeably higher than the corresponding value for the bulk T_g . This indicated that the PS chains near the interface were less mobile than those in the bulk. However, within experimental accuracy, this value was the same as that for PS-H at 392 K. In addition, the T_g for the 20-nm-thick film on silicon was determined by examining its thickness as a function of temperature via ellipsometry.⁴⁴ The values obtained for PS-H and PS-N were again identical (Supplementary Figure S2). Thus, it can be concluded that the segmental mobility in the interfacial region, at least within this depth range, was not restricted by the introduction of the functional end group.

Adsorption layer

Finally, the effect of the functional end group on the thickness of an adsorbed layer on a Si wafer was examined. The layer was difficult to remove even after washing the film with a good solvent.^{20,30,45,46} Figure 5 shows the thickness of the residual adsorbed layer on the substrate after rinsing with toluene, as determined by X-ray reflectivity as a function of the PS-N weight fraction in the film ($\phi_{\text{PS-N}}$). Typical X-ray reflectivity curves are shown in the inset. The reflectivity curve was well fitted with a simple one-layer electron density profile. The thickness of the adsorbed layer for PS-H was estimated to be 1.2 ± 0.1 nm, and this is in good agreement with the value reported elsewhere.³⁹ The layer became thicker with increasing $\phi_{\text{PS-N}}$ and reached 2.8 ± 0.3 nm for PS-N. These results clearly indicate that the incorporation of functional groups into the chains makes them more stable and difficult to remove from the substrate because of bond formation between the chains and the substrate.

Figure 6 shows schematic representations of possible chain conformations on solid substrates, proposed on the basis of our results and previous reports.^{20,21,47–53} As shown in Figure 6, polymer chains existing near the solid substrate can be roughly divided into two types: strongly and loosely adsorbed chains. To maximize polymer–substrate contacts, the former assume a conformation that is more flattened in comparison with the bulk random coil. Because such a chain possesses many segments (historically referred to as ‘trains’) that come into contact with the substrate, the functional end group may not have a significant impact on the structure and properties of the flattened chain. Conversely, the loosely adsorbed chains have fewer contact sites with the substrate. Given that the functionalized end also forms a contact point, it can be readily understood why the number density of loosely adsorbed chains increases with increasing $\phi_{\text{PS-N}}$ in the film: although the initial number density of loosely adsorbed chains at the surface is independent of $\phi_{\text{PS-N}}$, chains without the functional end can be partially washed out. The chains are finally collapsed in the film after the evaporation of toluene, leading to a residual layer thickness that is proportional to $\phi_{\text{PS-N}}$, as shown in Figure 5.

CONCLUSIONS

The effect of a functional end group, ω -N-(3-(dimethylamino)propyl) propylamide, on the stability of ultrathin PS films formed on a solid substrate was examined. When $\phi_{\text{PS-N}}$ was > 40 wt%, a 20-nm-thick film was stable even after annealing at a temperature above the bulk T_g . SFG spectroscopy indicated that the functionalized end of PS-N was aligned at the interface. Although the incorporation of functional

groups into the chains does not change the segmental dynamics at depths of ~ 20 nm, it makes them more stable and more difficult to remove from the substrate because of bond formation between the chains and the substrate. These findings will prove valuable in the design and construction of highly functionalized polymer interfaces with inorganic fillers.

CONFLICT OF INTEREST

The authors declare no conflict of interest.

ACKNOWLEDGEMENTS

This work was partly supported by Grant-in-Aids for Scientific Research on Innovative Areas ‘New Polymeric Materials Based on Element-Blocks’ (No. 15H00758) program and for Scientific Research (A) (No. 15H02183) from the Ministry of Education, Culture, Sports, Science and Technology, Japan. We are also grateful for support from JST SENTANKEISOKU (13A0004).

- 1 Yeh, J.-M. & Chang, K.-C. Polymer/layered silicate nanocomposite anticorrosive coatings. *J. Ind. Eng. Chem.* **14**, 275–291 (2008).
- 2 Cele, N. & Ray, S. S. Recent progress on nafion-based nanocomposite membranes for fuel cell applications. *Macromol. Mater. Eng.* **294**, 719–738 (2009).
- 3 Tripathi, B. P. & Shahi, V. K. Organic–inorganic nanocomposite polymer electrolyte membranes for fuel cell applications. *Prog. Polym. Sci.* **36**, 945–979 (2011).
- 4 Calebrese, C., Hui, L., Schadler, L. S. & Nelson, J. K. A review on the importance of nanocomposite processing to enhance electrical insulation. *IEEE Trans. Dielectr. Electr. Insul.* **18**, 938–945 (2011).
- 5 Feldman, D. Elastomer nanocomposite; properties. *J. Macromol. Sci., Part A* **49**, 784–793 (2012).
- 6 Lee, L. J., Zeng, C., Cao, X., Han, X., Shen, J. & Xu, G. Polymer nanocomposite foams. *Composit. Sci. Technol.* **65**, 2344–2363 (2005).
- 7 Holder, E., Tessler, N. & Rogach, A. L. Hybrid nanocomposite materials with organic and inorganic components for opto-electronic devices. *J. Mater. Chem.* **18**, 1064–1078 (2008).
- 8 Beecroft, L. L. & Ober, C. K. Nanocomposite materials for optical applications. *Chem. Mater.* **9**, 1302–1317 (1997).
- 9 Cong, H., Radosz, M., Towler, B. F. & Shen, Y. Polymer–inorganic nanocomposite membranes for gas separation. *Sep. Purif. Technol.* **55**, 281–291 (2007).
- 10 Porter, D., Metcalfe, E. & Thomas, M. J. K. Nanocomposite fire retardants – a review. *Fire Mater.* **24**, 45–52 (2000).
- 11 Schexnaider, P. & Schmidt, G. Nanocomposite polymer hydrogels. *Colloid Polym. Sci.* **287**, 1–11 (2009).
- 12 Haraguchi, K. Nanocomposite hydrogels. *Curr. Opin. Solid State Mater. Sci.* **11**, 47–54 (2007).
- 13 Stamm, M. *Polymer Surfaces and Interfaces: Characterization, Modification and Applications*, Springer-Verlag, Berlin Heidelberg, (2008).
- 14 Tsuruta, H., Fujii, Y., Kai, N., Kataoka, H., Ishizone, T., Doi, M., Morita, H. & Tanaka, K. Local conformation and relaxation of polystyrene at substrate interface. *Macromolecules* **45**, 4643–4649 (2012).
- 15 Shen, Y. R. Surface properties probed by second-harmonic and sum-frequency generation. *Nature* **337**, 519–525 (1989).
- 16 Chen, Z., Shen, Y. R. & Somorjai, G. A. Studies of polymer surfaces by sum frequency generation vibrational spectroscopy. *Annu. Rev. Phys. Chem.* **53**, 437–465 (2002).
- 17 Zhuang, X., Miranda, P. B., Kim, D. & Shen, Y. R. Mapping molecular orientation and conformation at interfaces by surface nonlinear optics. *Phys. Rev. B* **59**, 12632–12640 (1999).
- 18 Hirose, C., Akamatsu, N. & Domen, K. Formulas for the analysis of surface sum-frequency generation spectrum by CH stretching modes of methyl and methylene groups. *J. Chem. Phys.* **96**, 997–1004 (1992).
- 19 Napolitano, S. & Wübbenhorst, M. Effect of a reduced mobility layer on the interplay between molecular relaxations and diffusion-limited crystallization rate in ultrathin polymer films. *J. Phys. Chem. B* **111**, 5775–5780 (2007).
- 20 Gin, P., Jiang, N., Liang, C., Taniguchi, T., Akgun, B., Satija, S. K., Endoh, M. K. & Koga, T. Revealed architecture of adsorbed polymer chains at solid–polymer melt interfaces. *Phys. Rev. Lett.* **109**, 265501 (2012).
- 21 Jiang, N., Shang, J., Di, X., Endoh, M. K. & Koga, T. Formation mechanism of high-density, flattened polymer nanolayers adsorbed on planar solids. *Macromolecules* **47**, 2682–2689 (2014).
- 22 Tanaka, K., Tateishi, Y., Okada, Y. & Nagamura, T. Interfacial mobility of polymers on inorganic solids. *J. Phys. Chem. B* **113**, 4571–4577 (2009).
- 23 Kawaguchi, D., Tateishi, Y. & Tanaka, K. Time-resolved fluorescence analysis for dye-labeled polystyrene in thin films. *J. Non-Cryst. Solids* **407**, 284–287 (2015).
- 24 Paul, D. R. & Robeson, L. M. Polymer nanotechnology: nanocomposites. *Polymer* **49**, 3187–3204 (2008).
- 25 Zou, H., Wu, S. & Shen, J. Polymer/silica nanocomposites: preparation, characterization, properties, and applications. *Chem. Rev.* **108**, 3893–3957 (2008).

- 26 Kango, S., Kalia, S., Celli, A., Njuguna, J., Habibi, Y. & Kumar, R. Surface modification of inorganic nanoparticles for development of organic–inorganic nanocomposites—a review. *Prog. Polym. Sci.* **38**, 1232–1261 (2013).
- 27 Liu, J., Tanaka, T., Sivula, K., Alivisatos, A. P. & Fréchet, J. M. Employing end-functional polythiophene to control the morphology of nanocrystal–polymer composites in hybrid solar cells. *J. Am. Chem. Soc.* **126**, 6550–6551 (2004).
- 28 Liu, X., Zhao, S., Zhang, X., Li, X. & Bai, Y. Preparation, structure, and properties of solution-polymerized styrene-butadiene rubber with functionalized end-groups and its silica-filled composites. *Polymer* **55**, 1964–1976 (2014).
- 29 Reiter, G. Dewetting of thin polymer films. *Phys. Rev. Lett.* **68**, 75–78 (1992).
- 30 Reiter, G. Unstable thin polymer films: rupture and dewetting processes. *Langmuir* **9**, 1344–1351 (1993).
- 31 Henn, G., Bucknall, D. G., Stamm, M., Vanhoorne, P. & Jérôme, R. Chain end effects and dewetting in thin polymer films. *Macromolecules* **29**, 4305–4313 (1996).
- 32 Jones, R. A. L. & Richards, R. W. *Polymers at Surfaces and Interfaces* (Cambridge University Press, Cambridge, 1999).
- 33 Bäumchen, O. & Jacobs, K. Slip effects in polymer thin films. *J. Phys. Condens. Matter* **22**, 033102 (2010).
- 34 Paeng, K., Swallen, S. F. & Ediger, M. D. Direct measurement of molecular motion in freestanding polystyrene thin films. *J. Am. Chem. Soc.* **133**, 8444–8447 (2011).
- 35 Yang, Z., Fujii, Y., Lee, F. K., Lam, C.-H. & Tsui, O. K. C. Glass transition dynamics and surface layer mobility in unentangled polystyrene films. *Science* **328**, 1676–1679 (2010).
- 36 Stafford, C. M., Vogt, B. D., Harrison, C., Julthongpiput, D. & Huang, R. Elastic moduli of ultrathin amorphous polymer films. *Macromolecules* **39**, 5095–5099 (2006).
- 37 O'Connell, P. A. & McKenna, G. B. Rheological measurements of the thermoviscoelastic response of ultrathin polymer films. *Science* **307**, 1760–1763 (2005).
- 38 Ellison, C. J. & Torkelson, J. M. The distribution of glass-transition temperatures in nanoscopically confined glass formers. *Nat. Mater.* **2**, 695–700 (2003).
- 39 Fujii, Y., Yang, Z., Leach, J., Atarashi, H., Tanaka, K. & Tsui, O. K. C. Affinity of polystyrene films to hydrogen-passivated silicon and its relevance to the T_g of the films. *Macromolecules* **42**, 7418–7422 (2009).
- 40 Horinouchi, A., Yamada, N. L. & Tanaka, K. Aggregation states of polystyrene at nonsolvent interfaces. *Langmuir* **30**, 6565–6570 (2014).
- 41 Gautam, K. S., Schwab, A. D., Dhinojwala, A., Zhang, D., Dougal, S. M. & Yeganeh, M. S. Molecular structure of polystyrene at air/polymer and solid/polymer interfaces. *Phys. Rev. Lett.* **85**, 3854–3857 (2000).
- 42 Briggman, K. A., Stephenson, J. C., Wallace, W. E. & Richter, L. J. Absolute molecular orientational distribution of the polystyrene surface. *J. Phys. Chem. B* **105**, 2785–2791 (2001).
- 43 Curtis, A. D., Calchera, A. R., Asplund, M. C. & Patterson, J. E. Observation of sub-surface phenyl rings in polystyrene with vibrationally resonant sum-frequency generation. *Vib. Spectrosc.* **68**, 71–81 (2013).
- 44 Zhang, C., Fujii, Y. & Tanaka, K. Effect of long range interactions on the glass transition temperature of thin polystyrene films. *ACS Macro Lett.* **1**, 1317–1320 (2012).
- 45 Durning, C. J., O'Shaughnessy, B., Sawhney, U., Nguyen, D., Majewski, J. & Smith, G. S. Adsorption of poly(methyl methacrylate) melts on quartz. *Macromolecules* **32**, 6772–6781 (1999).
- 46 Hu, H. & Granick, S. Viscoelastic dynamics of confined polymer melts. *Science* **258**, 1339–1342 (1992).
- 47 Kaufman, S., Slichter, W. P. & Davis, D. D. Nuclear magnetic resonance study of rubber–carbon black interactions. *J. Polym. Sci. A Polym. Phys.* **9**, 829–839 (1971).
- 48 Ito, M., Nakamura, T. & Tanaka, K. Pulsed NMR study on the silica-filled rubber systems. *J. Appl. Polym. Sci.* **30**, 3493–3504 (1985).
- 49 Kirst, K. U., Kremer, F. & Litvinov, V. M. Broad-band dielectric spectroscopy on the molecular dynamics of bulk and adsorbed poly(dimethylsiloxane). *Macromolecules* **26**, 975–980 (1993).
- 50 Zhang, Y., Ge, S., Tang, B., Koga, T., Rafailovich, M. H., Sokolov, J. C., Peiffer, D. G., Li, Z., Dias, A. J., McElrath, K. O., Lin, M. Y., Satija, S. K., Urquhart, S. G., Ade, H. & Nguyen, D. Effect of carbon black and silica fillers in elastomer blends. *Macromolecules* **34**, 7056–7065 (2001).
- 51 Papon, A., Saalwächter, K., Schäler, K., Guy, L., Lequeux, F. & Montes, H. Low-field NMR investigations of nanocomposites: polymer dynamics and network effects. *Macromolecules* **44**, 913–922 (2011).
- 52 Papon, A., Montes, H., Hanafi, M., Lequeux, F., Guy, L. & Saalwächter, K. Glass-transition temperature gradient in nanocomposites: evidence from nuclear magnetic resonance and differential scanning calorimetry. *Phys. Rev. Lett.* **108**, 065702 (2012).
- 53 Choi, S.-S. & Ko, E. Novel test method to estimate bound rubber formation of silica-filled solution styrene-butadiene rubber compounds. *Polym. Test.* **40**, 170–177 (2014).

Supplementary Information accompanies the paper on Polymer Journal website (<http://www.nature.com/pj>)